Journal of
INTERNATIONAL
MEDICAL RESEARCH

Clinical analysis of percutaneous computed tomography–guided injection of cyanoacrylate for localization of 115 small pulmonary lesions in 113 asymptomatic patients

**Bing-Yang Huang[1],*, Jun-Jun Zhou[1],*,
Xiao-Yong Song[1],*, Ji-Hua Wu[2], Dong Zheng[3],
Xin-Ming Li[1] and Lu Li[1]** (iD)

Abstract

Objective: This study was performed to assess the clinical feasibility, safety, and effectiveness of a computed tomography (CT)–guided cyanoacrylate injection system and investigate the relationship between clinical features and pathologic characteristics of diminutive pulmonary lesions.
Methods: In total, 115 pulmonary nodules from 113 patients (63 female, 50 male) with a diameter of <20 mm were percutaneously localized with a CT-guided cyanoacrylate injection system and then resected.
Results: Of the pure ground-glass opacities (GGOs), 16.0% were atypical adenomatous hyperplasia (AAH), 18.7% were adenocarcinoma in situ (AIS), 49.3% were lung adenocarcinoma (ADC), and 16.0% were benign inflammatory fibrosis/fibrotic scars. Of the mixed GGOs, 18.2% were AAH, 22.7% were AIS, 22.7% were ADC, and 36.4% were benign lesions. Lesions of >10 mm and those located in relation to vessels were significantly more likely to be malignant. The success rate of both the cyanoacrylate injection system and video-assisted thoracoscopic surgery was 100% with no severe complications.

[1]Department of Cardiothoracic Surgery, The 306th Hospital of PLA, Chao-yang District, Beijing, People's Republic of China
[2]Department of Pathology, The 306th Hospital of PLA, Chao-yang District, Beijing, People's Republic of China
[3]Department of Radiology, The 306th Hospital of PLA, Chao-yang District, Beijing, People's Republic of China

*These authors contributed equally to this work and should be considered co-first authors.

Corresponding author:
Lu Li, Department of Cardiothoracic Surgery, The 306th Hospital of PLA, No. 9 An-xiang North Road, Chao-yang District, Beijing 100101, People's Republic of China.
Email: lilu_306@126.com

Conclusions: Preoperative localization of small pulmonary nodules using a cyanoacrylate injection system is a safe, simple, and useful technique.

Introduction

Advancements in high-resolution computed tomography (CT) during the past 10 years have allowed for the detection of increasingly more small pulmonary lesions using this technique. According to pulmonary malignancy screening trials, diminutive pulmonary lesions may be described as solid, pure ground-glass opacity (GGO), or mixed GGO.[1] Pathologically, GGO on CT images corresponds to atypical adenomatous hyperplasia (AAH) or early-stage adenocarcinoma (ADC) with a higher risk of malignancy compared with solid lesions.[2] However, the CT imaging features alone are inadequate for diagnosis, which is dependent upon a definitive pathologic diagnosis.[3] Video-assisted thoracoscopic surgery (VATS) can be performed for early biopsy and treatment of potentially cancerous tissue and helps to prolong the survival of patients with lung cancer.[4] Nevertheless, the application of VATS is restricted by the difficulty of positioning lung lesions that are small and adjacent to the pleura or nonsolid.[5,6]

Thus, various methods and tools have been developed to increase the success rate of localization of small lesions. Such techniques may be characterized as either preoperative or intraoperative. Preoperative techniques include metallic marker-based techniques, such as percutaneous placement of hook wires[7,8] and micro-coils[9,10] with or without a tail; liquid materials marker-based techniques, such as preoperative bronchoscopic placement of dyes[11] or percutaneous injection of dyes,[12] barium sulfate,[13] lipiodol,[14] radiotracers,[15] and indocyanine green fluorescence localization;[16] and needle puncture.[17] Intraoperative techniques include the use of intraoperative image-guided navigational systems[18] and ultrasound-guided surgery.[19] These localization methods have been proven useful, but several critical limitations restrict their wider applicability. For instance, radio-guided surgery involves radionuclides, which require the application of special installation equipment and radiation protection. Dyes used in staining diffuse easily, leading to excessive resection. Inflammatory responses caused by barium localization tend to influence the pathologic diagnosis. Lipiodol, a lipid-soluble radiopaque contrast medium, requires radioprotection throughout surgery, which is the main disadvantage of this method.

The high risks of pneumothorax and hemorrhage together with the possibility of dislodgement or migration lower the success rate of surgeries performed with hook-wire and micro-coil localization. Intraoperative techniques require more skill, equipment, or radionuclides. The technique of CT-guided percutaneous injection of cyanoacrylate has been used for many years. Yoshida et al.[20] first reported this localization technique for VATS in

1999, and it was further modified by Tyng et al.[21] in 2015. The technique was proven to be very useful, but its safety and efficacy were not fully evaluated.

The present study was performed to describe the use of a cyanoacrylate localization and injection system for nonpalpable lesions and show the feasibility, safety, and efficacy of this system. We also evaluated the correlation between the radiographic characteristics and pathologic features of the surgical specimens, which may help to elucidate the demographic characteristics of these small lesions, establish recommendations for clinical diagnosis and treatment, and improve cost-effectiveness.

Materials and methods

Patient selection

From August 2013 to February 2017, a series of consecutive asymptomatic patients who had been diagnosed with a peripheral pulmonary lesion by CT with indications for VATS resection at The 306th Hospital of PLA in Beijing were prospectively recruited for this study. The experimental protocol was approved by the Institutional Ethics Committee of The 306th Hospital (Approval number: J2012-10), and all patients provided written informed consent before enrollment.

Patient selection was based on the difficulty in CT-guided positioning of small pulmonary lesions with VATS. All decisions were finally made by discussion in a multidisciplinary team meeting involving thoracic surgeons, radiologists, oncologists, and pathologists. The factors considered in each case were nodule size, density, volume changes, CT features, and depth from the visceral pleural surface.

The inclusion criterion for this study was the appearance of a peripheral pulmonary nodule that had a transverse diameter of <2 cm, was located <3 cm from the visceral

pleura, and had a lesion density was classified as pure GGO, mixed GGO, or solid. A GGO was defined as a homogeneous hazy increase in density in the lung field that did not obscure the bronchiolovascular structures.

Some patients were followed up for >6 months by high-resolution CT (HRCT) before the operation, and surgical resection was performed when imaging changes appeared, such as an increase in size or the appearance of consolidation. The remaining patients underwent surgical resection without long-term follow-up because of a tumor history, smoking history, or continuous anxious state. All patients' sex, age, smoking history, cancer history, nodule location, size, CT characteristics, pathologic diagnosis, and immunohistochemistry results were recorded.

All lesions were detected with a 64-detector row dual-source HRCT machine (SOMATOM Definition Flash; Siemens, Erlangen, Germany) at the end of inspiration during one breath hold. The scan parameters were as follows: detector collimation, 64×0.6 mm; pitch, 1.4; section thickness and interval, 5.0 and 5.0 mm, respectively; scan time, 5–7 s; matrix, 512×512; field of view, 368 mm; 120 kVp; and 110 mAs. The CT images were reconstructed with a 0.7-mm thin layer and then processed in an MMWP 4.0 workstation (Siemens) including multiplanar recombination, surface recombination, and maximum density projection. The depth to the pleura was measured from the center of the lesion to the viscera.

CT-guided injection of cyanoacrylate and VATS

Lesion localization was completed with a 16-detector row scanner (Brilliance; Philips Medical Systems, Andover, MA, USA) at the end of inspiration during one breath hold. The scan parameters were as

follows: detector collimation, 16 mm × 1.5 mm; section thickness and interval, 5.0 and 5.0 mm, respectively; scan time, 5–7 s; matrix, 512 × 512; field of view, 350 mm; 120 kVp; and 200 mAs. Slices with a thickness of 5 mm were generated for each examination directly from the raw data.

The location equipment included a 17-gauge needle (Co-Axial Introducer Needle; Argon Medical Devices, Inc., Frisco, TX, USA) and cyanoacrylate (Baiyun Medical Glue, otologic and craniocerebral glue; Guangzhou Baiyun Medical Adhesive Co., Ltd., Guangzhou, China). Cyanoacrylate ($CH_2C(CN)COOC_8H_{17}$) is a rapidly curing medical adhesive product commonly used in endoscopic sclerotherapy[22] and otologic and craniocerebral operations.[23]

On the CT table, each patient was placed in a position that made the injection route as short as possible. Local anesthesia was followed by puncture of the injection site with a 17-gauge needle. We pushed the needle tip to the lung parenchyma and adjacent pulmonary lesion (generally <20 mm from the nodule) (Figure 1(a)) under CT guidance. Negative pressure was always maintained to guarantee that no blood was drawn into the needle; this avoided damage to the pulmonary vein

(Figure 1(b)). We injected 0.1 to 0.2 mL of cyanoacrylate and then immediately pulled the trocar needle out to confirm the location of the cyanoacrylate nodule relative to the target lesion by CT (Figure 1(c)).

VATS resection was performed after the injection. Upon exploration of the cyanoacrylate nodule present in the lung tissue (Figure 2(a)), a stapler was used to resect a wedge-shaped piece of lung tissue (Endo REACH; Reach Surgical, Inc., Tianjin, China). Resected tissues continued to be cut into smaller pieces. A fast-frozen section was immediately made after the cyanoacrylate nodule appeared and the pulmonary lesion was confirmed (Figure 2(b)). Pathologists performed a histological examination to verify the surgical margins. For lesions that were confirmed to be AAH or a benign neoplasm, we either ended the procedure (preferred) or proceeded to segmentectomy. For lesions that were diagnosed as carcinoma in patients without contraindications, we proceeded to lobectomy and lymph node dissection. The operation method was chosen with reference to the National Comprehensive Cancer Network lung cancer guidelines (version 1.2014). All specimens were reserved for permanent section with formalin fixation and paraffin
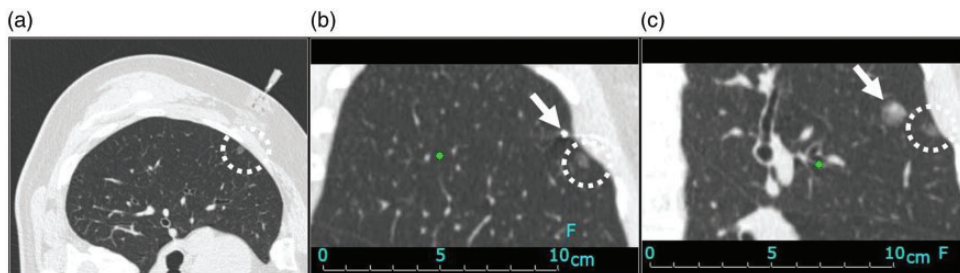
Figure 1. High-resolution computed tomography (CT) scans of pulmonary lesions. (a) Pure ground-glass opacity (GGO) lesion in a 60-year-old woman. Transverse lung-window thin-section CT scan shows 5.8-mm pure GGO nodule (circle) in the right upper lobe. This lesion was identified as atypical adenomatous hyperplasia (AAH) after wedge resection. (b) A 17-gauge puncture needle (Co-Axial Introducer Needle; Argon Medical Devices, Inc., Frisco, TX, USA) was inserted under CT guidance. The needle tip (arrow) was shown on the CT image. (c) The location of the cyanoacrylate nodule (arrow) and the target lesion were shown on the CT image.
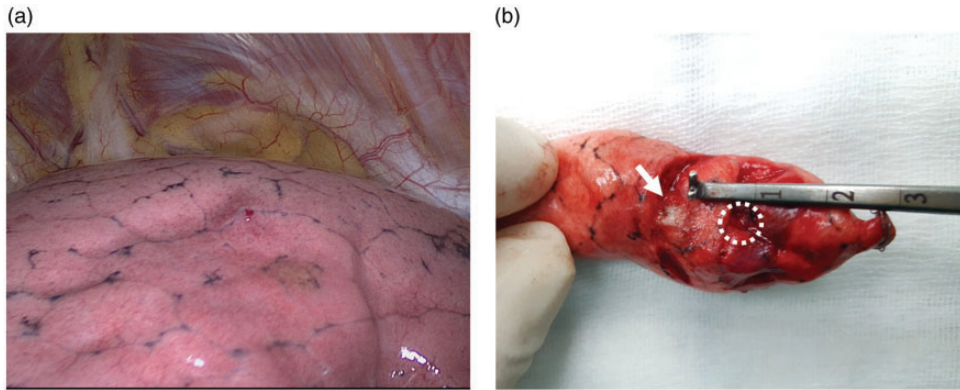
Figure 2. (a) Intraoperative exploration showed the cyanoacrylate nodule. Pulmonary hemorrhage (arrow) was useful in identification of the target lesion. (b) The location of the cyanoacrylate nodule (arrow) and the target lesion (circle) were shown after resection of a wedge-shaped piece of lung tissue. The distance between the cyanoacrylate nodule and target lesion was 10 mm.

embedding for the final diagnosis. Every diagnosis was confirmed by two pathologists.

Data collection and statistical analysis

All statistical analyses were completed with SPSS version 19.0 (IBM Corp., Armonk, NY, USA). All variables, including the clinical and radiologic characteristics, were analyzed by the logistic regression method. A p-value of <0.05 was considered statistically significant. Numerical data were compared by an independent-samples t-test or one-way analysis of variance. Categorical data were analyzed by Pearson's χ^2 test or Fisher's exact test.

Results

General characteristics of pulmonary lesions

In total, 113 consecutive asymptomatic patients were included in the study (50 men and 63 women; mean age, 59.3 ± 11.9 years; range, 25–83 years). Thirty-six patients had a history of smoking and 25 had a history of cancer (Table 1). Thirty-two patients with lesions of <8 mm were

followed up for >6 months by HRCT, and the patterns of imaging changes during the follow-up were categorized into four types: type 1, pure GGO that increased in size with no consolidation ($n = 12$); type 2, consolidation within a pure GGO with or without an increase in size ($n = 9$); type 3, mixed GGO that increased in size and exhibited consolidation ($n = 7$); and type 4, consolidation without pure GGO in solid nodules ($n = 4$). The average follow-up interval from the first HRCT scan to the scan before the operation was 13 months (range, 6–32 months). The remaining 81 patients underwent surgical resection without long-term follow-up.

All 113 patients underwent CT-guided injection of cyanoacrylate for the localization of 115 pulmonary lesions. Two patients had two lesions and underwent the localization procedure for each lesion at the same time. The distance from the peripheral edge of the nodule to the nearest pleural surface was determined on CT images and ranged from 3 to 20 mm (average, 11 mm). The mean long axial dimension of all lesions on CT was 9.4 ± 3.5 mm (range, 3.5–18 mm). Malignant lung tissue had a significantly larger diameter (10.6 ± 2.9 mm) than

Table 1. Clinical characteristics of pulmonary lesions with different pathologic diagnoses.

Pathology of Pulmonary Lesions

Characteristics	Benign lesions	AAH	AIS	ADC	p value
Age, years	58.3 ± 13.1	56.8 ± 14.8	57.3 ± 11.7	61.5 ± 10.4	0.621
Sex					0.089
Female	11	12	12	28	
Male	19	4	7	21	
Smoking history					0.598
Yes	11	3	5	17	
No	19	13	14	32	
Cancer history					0.503
Yes	4	5	4	12	
No	26	11	15	37	
Location					0.842
Left upper lobe	11	5	2	15	
Left lower lobe	7	4	0	8	
Right upper lobe	5	4	9	14	
Right lower lobe	6	3	6	4	
Right middle lobe	1	0	2	8	

Data are presented as mean ± standard deviation or n.
AAH, atypical adenomatous hyperplasia; AIS, adenocarcinoma in situ; ADC, lung adenocarcinoma.

adenocarcinoma in situ (AIS) (9.0 ± 2.4 mm), AAH (8.4 ± 4.1 mm), and benign lesions (8.1 ± 3.8 mm) ($p < 0.05$) on CT (Table 2). No significant difference was found in age, sex, cancer history, smoking history, or lesion location among these groups.

Pathologic analysis of different radiologic pulmonary lesions

Of the targeted lesions, 75 (65.2%) were pure GGOs, 22 (19.1%) were mixed (partially solid) GGOs, and 18 (15.7%) were solid nodules. The mean tumor size of pure GGOs, mixed GGOs, and solid nodules was 9.6 ± 3.5, 8.0 ± 3.4, and 9.2 ± 2.8 mm, respectively.

Pathologically, of the 75 pure GGOs, 12 (16.0%) were benign lesions, 12 (16.0%) were AAH, 14 (18.7%) were AIS, and 37 (49.3%) were ADC (Figure 3(a)). Nineteen and 40 of the 68 lung cancers were classified as stage 0 and IA, respectively. The other

9 lung cancers with pleural involvement were classified as stage Ib. One male patient with two pure GGO lesions was diagnosed with AAH and ADC, respectively. One female patient with a pure GGO lesion and a mixed GGO lesion was diagnosed with AIS and ADC, respectively. No local recurrence or metastasis was observed during the follow-up period of 0.5 to 2 years. The mean tumor size of AAH, AIS, ADC, and benign lesions was 9.5 ± 3.9 mm (range, 4.3–16.5 mm), 9.1 ± 2.4 mm (range, 4.8–13 mm), 10.4 ± 3.2 mm (range, 5.5–17.1 mm), and 7.7 ± 4.3 mm (range, 3.5–18 mm), respectively. ADC was significantly larger than benign lesions ($p = 0.025$). Of the 22 mixed GGOs, 8 (36.4%) were benign lesions, 4 (18.2%) were AAH, 5 (22.7%) were AIS, and 5 (22.7%) were ADC. The mean tumor size of AAH, AIS, ADC, and benign lesions was 5.2 ± 2.4 mm (range, 4–8.7 mm), 8.6 ± 2.4 mm (range, 6–11 mm), 11.0 ± 3.2 mm (range, 8–15.8 mm), and 7.2 ± 3.3 mm (range, 3.5–13 mm),

Table 2. Tumor size on CT scan versus pathological diagnosis.

Pathologic diagnosis	n	CT lesion size (mm)	Independent-samples t-test
Pure GGO			
Benign lesions	12	7.7 ± 4.3 (3.5–18)	Benign lesions vs. AAH: p = 0.291
AAH	12	9.5 ± 3.9 (4.3–16.5)	Benign lesions vs. AIS: p = 0.282
AIS	14	9.1 ± 2.4 (4.8–13)	**Benign lesions vs. ADC: p = 0.025**
ADC	37	10.4 ± 3.2 (5.5–17.1)	AAH vs. AIS: p = 0.786
Total	75	9.6 ± 3.5 (3.5–18)	AAH vs. ADC: p = 0.445
			AIS vs. ADC: p = 0.206
Mixed GGO			
Benign lesions	8	7.2 ± 3.3 (3.5–13)	Benign lesions vs. AAH: p = 0.301
AAH	4	5.2 ± 2.4 (4–8.7)	Benign lesions vs. AIS: p = 0.443
AIS	5	8.6 ± 2.4 (6–11)	Benign lesions vs. ADC: p = 0.069
ADC	5	11.0 ± 3.2 (8–15.8)	AAH vs. AIS: p = 0.069
Total	22	8.0 ± 3.4 (3.5–15.8)	**AAH vs. ADC: p = 0.019**
			AIS vs. ADC: p = 0.216
Solid nodules			
Benign lesions	10	8.3 ± 3.5 (4.8–13.3)	Benign lesions vs. ADC: p = 0.062
ADC	7	11.1 ± 0.9 (5.1–14.4)	
Total	17	9.2 ± 2.8 (4.8–14.4)	
Total			
Benign lesions	30	8.1 ± 3.8 (3.5–18)	Benign lesions vs. AAH: p = 0.772
AAH	16	8.4 ± 4.1 (4–16.5)	Benign lesions vs. AIS: p = 0.344
AIS	19	9 ± 2.4 (4.8–13)	**Benign lesions vs. ADC: p = 0.002**
ADC	49	10.6 ± 2.9 (5.1–17.1)	AAH vs. AIS: p = 0.597
All lesions	115	9.42 ± 3.5 (3.5–18)	**AAH vs. ADC: p = 0.027**
			AIS vs. ADC: p = 0.037

Data are presented as mean ± standard deviation (range).
CT, computed tomography; GGO, ground-glass opacity; AAH, atypical adenomatous hyperplasia; AIS, adenocarcinoma in situ; ADC, lung adenocarcinoma.
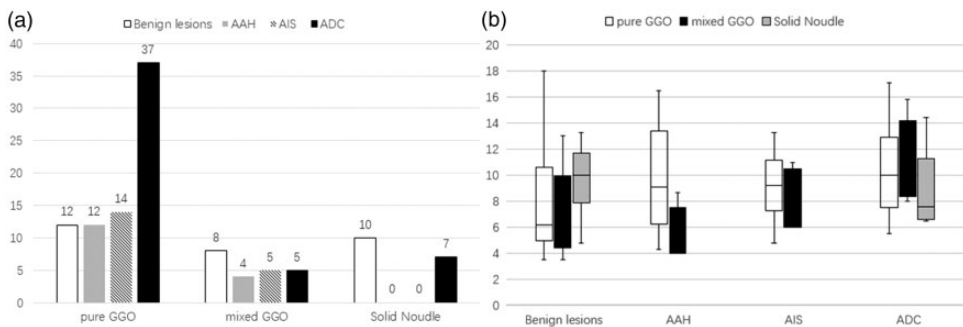
Figure 3. Pathologic distribution and size of lesions. (a) Pathologic distribution of lesions. (b) Size of nodules. AAH, atypical adenomatous hyperplasia; AIS, adenocarcinoma in situ; ADC, lung adenocarcinoma; GGO, ground-glass opacity.

respectively. ADC was significantly larger than AAH (p = 0.019). Of the 18 solid nodules, 10 (55.6%) were benign lesions, 7 (38.9%) were ADC, and 1 (5.6%) was a carcinoid tumor; no AIS or AAH was observed among the solid nodules. The mean tumor size of ADC and benign lesions was 11.1 ± 0.9 mm (range, 5.1–14.4 mm) and 8.3 ± 3.5 mm (range, 4.8–13.3 mm), respectively (Figure 3(b)).

Remarkable differences were found in the pathologic distribution among these different types of lesions. Compared with solid nodules, pure GGO and mixed GGO lesions were more likely to be malignant (p < 0.05). The following radiological characteristics were found to be significantly different among ADC, AIS, AAH, and benign lesions: GGO density (p = 0.000), lesion shape (p = 0.006), air bronchograms (p = 0.028), pleural tags (p = 0.037), lesions of >10 mm (p = 0.01), and relationship to vessels (p = 0.003). The patients' age, lesion border, lesion margin, and presence of bubble lucency were not predictive for the pathologic diagnosis (Table 3).

Four patterns of radiological changes were found during the initial CT examination, as described above. Type 1 comprised six cases of AAH, four of AIS, and two of ADC, and the median follow-up time was 15 months (range, 6–25 months). Type 2 comprised two cases of AAH, five of AIS, and two of ADC, and the median follow-up time was 12 months (range, 6–32 months). Type 3 comprised one case of AAH, four of AIS, and two of ADC, and the median follow-up time was 11 months (range, 6–28 months). Finally, type 4 comprised no cases of AAH or AIS, three of ADC, and one of tuberculosis, and the median follow-up time was 9 months (range, 6–22 months).

Complications

Injection of cyanoacrylate resulted in successful localization of all lesions during the operation. Additionally, VATS was successfully performed in all patients. Partial pneumothorax (<10% on CT scans) was detected in 8.0% (9/113) of patients and was self-limiting. Thoracic drainage was performed in 0.8% (1/113) of patients. Moderate pain (visual analogue scale scores of 3–6) occurred in 5.3% (6/113) of patients. Postoperative coughing occurred in 4.4% (5/113) of patients and improved after treatment. No pulmonary hemorrhage occurred.

Discussion

We have performed the largest study to date investigating the clinical feasibility, safety, and effectiveness of CT-guided injection of cyanoacrylate for lesion localization. We examined 115 lung lesions after CT-guided injection of cyanoacrylate, and VATS was conducted for diagnosis or treatment. Percutaneous CT-guided injection of cyanoacrylate does not require intraoperative fluoroscopy for detection of targets, and it facilitates easy resection of small lung lesions.

Although this was a single-center study, it produced some interesting and clinically valuable findings. The multivariate analysis showed no significant correlation between the risk of malignancy and a history of smoking or cancer. We plan to expand the sample size in a future study to further confirm this result. We also observed that patients without a history of smoking had a higher risk of AAH and AIS, which contrasts the findings of previous research.[24] This difference might be ascribed to exposure to other risk factors for lung cancer in nonsmoking patients, such as passive smoking or cooking fumes.[25] The patterns of imaging changes within the follow-up period of our study were divided into four types. Type 4 tended to occur sooner after the initial CT examination. Types 1 and 2 tended to occur in patients with AAH and

Table 3. CT imaging characteristics of pulmonary lesions with different pathologic diagnoses.

Pathology of Pulmonary Lesions

Pathology	Benign lesions				AAH			AIS			ADC				p
CT image	Pure GGO	Mixed GGO	SN	T	Pure GGO	Mixed GGO	T	Pure GGO	Mixed GGO	T	Pure GGO	Mixed GGO	SN	T	
Number	12	8	10	30	12	4	16	14	5	19	37	5	7	49	0.000
Shape															**0.006**
Round	5	1	6	12	6	2	8	6	2	8	15	3	1	19	
Oval	3	4	1	8	2	1	3	6	2	8	9	0	2	11	
Irregular	4	3	3	10	4	1	5	2	1	3	13	2	4	19	
Border															0.361
Undefined	0	4	3	7	3	2	5	4	3	7	13	4	4	21	
Well-defined	12	4	7	23	9	2	11	10	2	12	24	1	3	28	
Margin															0.202
Smooth	11	3	6	20	8	3	11	12	3	15	22	1	3	26	
Lobulated	0	0	1	1	0	0	0	0	0	0	0	0	0	0	
Spiculated	1	5	3	9	4	1	5	2	2	4	15	4	4	23	
Surrounding vasculature															**0.003**
Pass through	2	5	3	10	5	1	6	10	3	13	10	2	4	16	
Convergence	2	0	0	2	0	0	0	2	2	4	7	2	1	10	
Unrelated	8	3	7	18	7	3	10	2	0	2	20	1	2	23	
Air bron	2	0	2	4	2	1	3	2	1	3	1	0	0	1	**0.028**
Bubble lucency	2	0	1	3	2	1	3	2	1	3	7	2	0	9	0.783
Pleural tag	0	1	1	2	0	0	0	0	0	0	6	1	2	9	**0.037**
CT size															**0.01**
≤10 mm	10	7	8	25	7	4	11	9	4	13	19	3	1	23	
10–20 mm	2	1	2	5	5	0	5	5	1	6	18	2	6	26	
Age															0.14
≤60 y	6	7	5	18	9	4	13	5	5	10	17	4	3	24	
>60 y	6	1	5	12	3	0	3	9	0	9	20	1	4	25	

CT, computed tomography; GGO, ground-glass opacity; AAH, atypical adenomatous hyperplasia; AIS, adenocarcinoma in situ; ADC, lung adenocarcinoma; T, total; SN, solid nodule; bron, bronchogram.

AIS, while type 4 tended to occur in those with ADC. These results are consistent with a study reported by Yoshida et al.[26] Lesions with type 1 and type 2 changes might progress to type 3, and type 4 might be a separate development pattern that occurs in the long term.

In our study, more than three-quarters of the pure GGO lesions were lung cancer, including ADC and AIS, while half of the pure GGO lesions were diagnosed as invasive ADC. Approximately half of the mixed GGO lesions were ADC and AIS. The percentage of invasive ADC among pure GGOs and the percentage of ADC/AIS among mixed GGOs were relatively high, which we attributed to three factors. First, the inclusion criterion was relatively strict; only patients with a nodule that had gradually increased in size or showed potentially malignant features were included. Second, among the pure GGOs, the size of ADC was larger than that of the other subtypes. Third, the relatively small sample size of the mixed GGOs (n = 22) might have influenced the results. Previous studies have suggested that the presence of a persistent GGO lesion is strongly correlated with a neoplastic condition, such as AAH or early ADC.[27,28] Similar results were reported by Xu et al.[8] and Li et al.,[29] whose findings were also consistent with those of our study.

In 2015, Xu et al.[8] described the use of a hook wire system for preoperative localization of small pulmonary nodules. They also found that subsolid lung nodules with a diameter >10 mm were more likely to be malignant. In a study with a small sample size, Ohtsuka et al.[30] reported that all lesions of >10 mm were bronchioloalveolar carcinoma. Pure GGO and mixed GGO lesions had a greater tendency to be malignant, and the mean lesion size increased in the order of benign lesions, AAH, AIS, and ADC. Because invasive lesions are expected to grow with time (the mean volume-doubling time of a GGO lesion is

approximately 800 days), such lesions should be monitored by CT screening. Patients with lesions that show a predominant GGO component and are >10 mm in diameter should be carefully monitored to ensure timely active treatment. We suggest that patients with small solid nodules (<10 mm) with a round, well-defined border and smooth margin should be followed up regularly instead of undergoing immediate surgical resection.

According to the present study, the complications related to cyanoacrylate injection are few and mild. The main concern regarding the use of adhesive in the lung is that it is very likely to generate embolism. Jun et al.[31] and Harunarashid et al.[32] reported the occurrence of brain and lung embolism among patients who underwent endoscopic sclerotherapy of esophagogastric varices with isobutyl-2-cyanoacrylate. The symptoms were not severe, however, and the patients recovered in a few weeks. Although no report has described the use of Histoacryl, it is crucial to avoid vascular damage when performing invasive procedures and to prevent crushing of the cyanoacrylate nodule during VATS wedge resection. The surgeon should also confirm that no blood is withdrawn by retracting the syringe piston before injecting the adhesive.

This study has several limitations. First, the histologic subtypes of ADC were not recorded. Second, although the sample size of this study was large, the sample size of each subtype (mixed GGOs, n = 22; solid nodules, n = 18) was still small, which might have led to bias. Further studies are needed to thoroughly elucidate the features of small pulmonary nodules.

In conclusion, percutaneous injection of cyanoacrylate for preoperative localization of small pulmonary lesions yielded high success rates and low complication rates. Among all pulmonary nodules of ≤20 mm, GGOs tended to be malignant and small solid nodules were more likely to be

benign. Pulmonary lesions with a diameter of >10 mm were more likely to be malignant. Preoperative CT-guided percutaneous injection of cyanoacrylate and VATS can be widely performed for the surgical treatment of small lung lesions.

Declaration of conflicting interest

The authors declare that there is no conflict of interest.

Funding

ORCID iD

Lu Li http://orcid.org/0000-0002-0476-1881

References

1. Naidich DP, Bankier AA, MacMahon H, et al. Recommendations for the management of subsolid pulmonary nodules detected at CT: a statement from the Fleischner Society. *Radiology* 2013; 266: 304–317.

2. Hiramatsu M, Inagaki T, Inagaki T, et al. Pulmonary ground-glass opacity (GGO) lesions-large size and a history of lung cancer are risk factors for growth. *J Thorac Oncol* 2008; 3: 1245–1250.

3. Dai C, Ren Y, Xie H, et al. Clinical and radiological features of synchronous pure ground-glass nodules observed along with operable non-small cell lung cancer. *J Surg Oncol* 2016; 113: 738–744.

4. Congregado M, Merchan RJ, Gallardo G, et al. Video-assisted thoracic surgery (VATS) lobectomy: 13 years' experience. *Surg Endosc* 2008; 22: 1852–1857.

5. Park CH, Han K, Hur J, et al. Comparative effectiveness and safety of pre-operative lung localization for pulmonary nodules: a systematic review and meta-analysis. *Chest* 2017; 151: 316–328.

6. Nakashima S, Watanabe A, Obama T, et al. Need for preoperative computed tomography-guided localization in video-assisted thoracoscopic surgery pulmonary resections of metastatic pulmonary nodules. *Ann Thorac Surg* 2010; 89: 212–218.

7. Miyoshi K, Toyooka S, Gobara H, et al. Clinical outcomes of short hook wire and suture marking system in thoracoscopic resection for pulmonary nodules. *Eur J Cardiothorac Surg* 2009; 36: 378–382.

8. Xu X, Yao Y, Shen Y, et al. Clinical analysis of percutaneous computed tomography-guided hook wire localization of 168 small pulmonary nodules. *Ann Thorac Surg* 2015; 100: 1861–1867.

9. Su TH, Fan YF, Jin L, et al. CT-guided localization of small pulmonary nodules using adjacent microcoil implantation prior to video-assisted thoracoscopic surgical resection. *Eur Radiol* 2015; 25: 2627–2633.

10. Powell TI, Jangra D, Clifton JC, et al. Peripheral lung nodules: fluoroscopically guided video-assisted thoracoscopic resection after computed tomography-guided localization using platinum microcoils. *Ann Surg* 2004; 240: 481–488.

11. Endo M, Kotani Y, Satouchi M, et al. CT fluoroscopy-guided bronchoscopic dye marking for resection of small peripheral pulmonary nodules. *Chest* 2004; 125: 1747–1752.

12. Findik G, Demiröz SM, Apaydın SMK, et al. Computed tomography-guided methylene blue labeling prior to thoracoscopic resection of small deeply placed pulmonary nodules, do we really need palpation? *Thorac Cardiovasc Surg* 2017; 65: 387–391.

13. Lee NK, Park CM, Kang CH, et al. CT-guided percutaneous transthoracic localization of pulmonary nodules prior to video-assisted thoracoscopic surgery using barium suspension. *Korean J Radiol* 2012; 13: 694–701.

14. Watanabe K, Nomori H, Ohtsuka T, et al. Usefulness and complications of computed tomography-guided lipiodol marking for fluoroscopy-assisted thoracoscopic resection of small pulmonary nodules: experience with 174 nodules. *J Thorac Cardiovasc Surg* 2006; 132: 320–324.

15. Bellomi M, Veronesi G and Trifirò G. Computed tomography-guided preoperative radiotracer localization of nonpalpable lung nodules. *Ann Thorac Surg* 2010; 90: 1759–1765.

16. Ujiie H, Kato T, Hu HP, et al. A novel minimally invasive near-infrared thoracoscopic localization technique of small pulmonary nodules: a phase I feasibility trial. *J Thorac Cardiovasc Surg* 2017; 154: 702–711.

17. Hsu HH, Shen CH, Tsai WC, et al. Localization of nonpalpable pulmonary nodules using CT-guided needle puncture. *World J Surg Oncol* 2015; 13: 248.

18. Silvestri GA, Herth FJ, Keast T, et al. Feasibility and safety of bronchoscopic transparenchymal nodule access in canines: a new real-time image-guided approach to lung lesions. *Chest* 2014; 145: 833–838.

19. Yamamoto M, Takeo M, Meguro, et al. Sonographic evaluation for peripheral pulmonary nodules during video-assisted thoracoscopic surgery. *Surg Endosc* 2003; 17: 825–827.

20. Yoshida J, Nagai K, Nishimura M, et al. Computed tomography-fluoroscopy guided injection of cyanoacrylate to mark a pulmonary nodule for thoracoscopic resection. *Jpn J Thorac Cardiovasc Surg* 1999; 47: 210–213.

21. Tyng CJ, Nogueira VH, Bitencourt AG, et al. Computed tomographically guided injection of cyanoacrylate in association with preoperative radioguided occult lesion localization of ground-glass opacities. *Ann Thorac Surg* 2015; 99: 1838–1840.

22. Ríos Castellanos E, Seron P, Gisbert JP, et al. Endoscopic injection of cyanoacrylate glue versus other endoscopic procedures for acute bleeding gastric varices in people with portal hypertension. *Cochrane Database Syst Rev* 2015; 5: CD010180.

23. Maw JL, Kartush JM, Bouchard K, et al. Octylcyanoacrylate: a new medical-grade adhesive for otologic surgery. *Am J Otol* 2000; 21: 310–314.

24. Alberg AJ, Brock MV, Ford JG, et al. Epidemiology of lung cancer: diagnosis and management of lung cancer, 3rd ed: American College of Chest Physicians evidence-based clinical practice guidelines. *Chest* 2013; 143: e1S–e29S.

25. Jemal A, Bray F, Center MM, et al. Global cancer statistics. *CA Cancer J Clin* 2011; 61: 69–90.

26. Yoshida Y, Kokubu A, Suzuki K, et al. Molecular markers and changes of computed tomography appearance in lung adenocarcinoma with ground-glass opacity. *Jpn J Clin Oncol* 2007; 37: 907–912.

27. Henschke CI, Yankelevitz DF, Mirtcheva R, et al. CT screening for lung cancer: frequency and significance of part-solid and nonsolid nodules. *AJR Am J Roentgenol* 2002; 178: 1053–1057.

28. Park CM, Goo JM, Lee HJ, et al. Nodular ground-glass opacity at thin-section CT: histologic correlation and evaluation of change at follow-up. *Radiographics* 2007; 27: 391–408.

29. Li F, Sone S, Abe H, et al. Malignant versus benign nodules at CT screening for lung cancer: comparison of thin-section CT findings. *Radiology* 2004; 233: 793–798.

30. Ohtsuka T, Watanabe K, Kaji M, et al. A clinicopathological study of resected pulmonary nodules with focal pure ground-glass opacity. *Eur J Cardiothorac Surg* 2006; 30: 160–163.

31. Jun CH, Kim KR, Yoon JH, et al. Clinical outcomes of gastric variceal obliteration using N-butyl-2-cyanoacrylate in patients with acute gastric variceal hemorrhage. *Korean J Intern Med* 2014; 29: 437–444.

32. Harunarashid H, Lily S, Rozman Z, et al. Pulmonary embolism following histoacryl glue embolization for a large thigh arteriovenous malformation. *Clin Ter* 2012; 163: 393–395.